The Journal of Engineering Geology, Vol.16, No.2, June, 2006, pp. 179-187

A Study on the Source Mechanism of Micro-crack by Radiation Pattern

Sang-Eun Lee*

Sambo Engineering Co., Ltd.

방사형식에 의한 미소균열의 파괴메커니즘에 관한 연구

이 상 은*

(주)삼보기술단

Two specimens of mortar containing artificial slit and Geochang granite containing the straight notch were selected to be used in this research. Source mechanism of micro-crack by radiation pattern based on dislocation theory was estimated by the first motion of longitudinal wave and spatial distribution between the location of transducers for monitoring acoustic emission and source coordinates determined by the application of the least square method. Result of analysis showed that the orientation of dislocation surfaces due to shear dislocation and tensile dislocation squares considerably with crack direction visually observed. The ultimate goal of this study is to provide fundamental information for source mechanism of micro-crack within materials.

Key words : Source mechanism, Micro-crack, Radiation pattern, Dislocation

인공적인 슬릿을 형성한 모르타르와 노치를 형성한 화강암 시편이 이 연구를 위해 사용되었다. 전위이론을 토대로 방사형식에 의한 미소균열의 파괴 메커니즘이 변환기에 탐지된 종파의 초동, 모니터링을 위한 변환기의 위치와 최소자승법 적용에 의해 결정된 파괴원 위치 사이의 공간적인 분포에 의해 평가되었다. 해석결과 전위면의 방위는 육안으로 관찰된 시편의 균열방향과 비교적 잘 일치하였다. 이 연구의 궁극적인 목적은 암석재료내 미소균열의 파괴 메커니즘에 관한 기본적인 정보를 제공하는데 있다.

주요어 : 파괴 메커니즘, 미소균열, 방사형식, 전위

Introduction

Nondestructive test methods such as ultrasonic test can only detect the location and magnitude of existing fault, while acoustic emission is particularly useful in the point that it can prevent accident by monitoring dynamic behavior within the structure - such as the magnitude of damage of fault may cause and the development of cracks.

Research in Korea on acoustic emission has been attempted mainly for metallic and composite materials since twenty old years ago. There are only thesis on rock as a result of research in laboratory. Heralded reports of them are supplementary measure on hydraulic fracturing method by Kim (1990), rock properties in uniaxial compression test by Ko (1983), and three-dimensional source location considering anisotropic velocity by Lee (1996). No search has as yet been attempted for source mechanism of micro-crack by means of acoustic emission in rock.

Therefore, with adaptation of dislocation theory at radiation pattern and by analyzing spatial distribution of source location determined from the

*Corresponding author: lee9367@hanmail.net

application of least sqo7are method by Leighton and Duvall (1972), transducers for monitoring acoustic emission, and the pattern of first motion of longitudinal wave, a study has been done on source mechanism of micro-crack i. e. characteristics of material in relation to tensile crack and shear crack due to dislocation tensile and shear dislocation.

Basic theory

Elastic wave is primarily classified as the longitudinal wave, transverse wave and surface wave, and each such wave at certain occasions takes form of its inherent amplitude respectively. These amplitudes when they distribute in three dimension can them be classified as dislocation by point force, tensile or shear. Crack pattern resulted within the material corresponds to the dislocation pattern caused i. e. tensile crack or shear crack to tensile dislocation or shear dislocation respectively. In this study only the first motion of longitudinal wave which makes the first reaching during propagating period, was taken into consideration when reviewing dislocation theory by Ohtsu (1983), Aki and Richard (1980) etc.

Dislocation by point force

Point force $f_i(\tau)$ can be represented as eq. (1).

$$f_i(\tau) = F \cdot n_i \cdot H(\tau) \tag{1}$$

F : magnitude of point force
n_i : direction of point force
$H(\tau)$: function of Heviside step

Summation of the same directional vector components (γ) of detecting points at the source of dislocation makes up $\gamma_k\gamma_k = 1$. Therefore, dispalcement to k direction (u_k) is represented as eq. (2).

$$u_k\gamma_k = \frac{F}{4\pi\rho v_p^2}\cdot\frac{1}{r}\cdot(\gamma_i u_i)H(t-r/v_p) \tag{2}$$

Eq. (2) shows displacement component to the direction connecting point ξ and point x provided that x is any arrival point of longitudinal wave when force F is applied to the point of dislocation

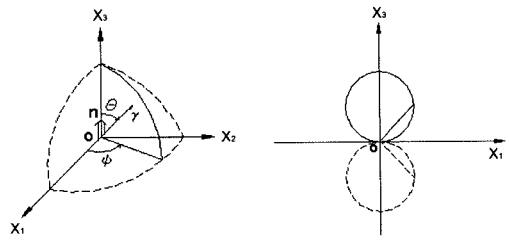

(a) dislocation model (b) radiation pattern

Fig. 1. Dislocation model for the point force and its radiation pattern.

source ξ. Eliminating the components in above equation relating applied force, transmitting medium and distance, remainder is $\gamma_i n_i$ which refer to amplitude related to spatial positioning.

When point force is applied from 0 to x_3 direction as shown in Fig. 1, if γ=(sinθcosθ, sinθsinϕ, cosθ) is spherical coordinate system, n=(0,0,1). Therefore, displacement by radiation pattern of longitudinal wave u is represented as eq. (3).

$$u_{(p)} = \gamma_i n_i = \cos\theta \tag{3}$$

The displacement component of longitudinal wave at eq. (2) is as represented as eq. (4)

$$u_{k(P)} = \frac{F}{4\pi\rho v_p^2}\cdot\frac{1}{r}\cdot\gamma_k\gamma_i n_i \tag{4}$$

Amplitude detected to output of transducers since transducers for monitoring acoustic emission detect only the component of normal direction can be represented as eq. (5).

$$u_{k(P)}{}^{(i)}\mu_k^{(i)} = \frac{F}{4\pi\rho v_p^2}\cdot\frac{1}{r^{(i)}}\{\gamma_k^{(i)}\mu_k^{(i)}\}\cdot\{\gamma_i^{(i)}n_i\} \tag{5}$$
$$(i = 1, 2, \cdots, N)$$

First term related to the magnitude of point force and the physical properties of transmitting medium is represented with A, second term can be obtained from geometric relation between detecting point and source coordinates, and third term related to applied direction of point force.

Meanwhile, correction of amplitude at detecting point $R^{(i)}$ is as follows.

$$R^{(i)}=\frac{u_{k(P)}{}^{(i)}\mu_k^{(i)}}{\frac{1}{r^{(i)}}\{\gamma_k^{(i)}\mu_k^{(i)}\}}=A\gamma_l^{(i)}n_l$$
$$=\gamma_1^{(i)}(An_1)+\gamma_2^{(i)}(An_2)+\gamma_3^{(i)}(An_3) \quad (i=1, 2, \cdots, N) \tag{6}$$

Eq. (6) is simultaneous equation of the number of detecting point having the unknown An_1, An_2, and An_3. Therefore, An_1, An_2, and An_3 can be determined from amplitudes detected by transducers more than three channels and accurate source coordinates.

Shear dislocation

Shear dislocation is represented as eq. (7).

$$[u_i(\tau)]=U\cdot n_i\cdot H(\tau) \tag{7}$$

When normal vector on the surface of dislocation v and directional vector of dislocation n meets perpendicularly, $v_in_i=0$. Therefore, the component of longitudinal wave of shear dislocation is represented as eq. (8).

$$u_k\gamma_k=\frac{\mu\cdot U}{4\pi\rho v_p^2}\cdot\frac{1}{r}\cdot 2(\gamma_in_i)(\gamma_iv_i)\delta\left(t-\frac{r}{v_p}\right) \tag{8}$$

Shear dislocation and its radiation pattern is as shown in Fig. 2, and radiation pattern of longitudianl wave is represented as eq. (9). when v=(0, 0, 1), n=(1, 0, 0)

$$u_{(p)}=2(\gamma_in_i)(\gamma_iv_i)=2\sin\theta\cos\theta\cos\phi=\sin2\theta\cos\phi \tag{9}$$

Amplitude of the first motion of longitudinal wave as well in case of dislocation of point force is as eq. (10).

$$u_{k(P)}{}^{(i)}\mu_k^{(i)}=\frac{2\mu\cdot U}{4\pi\rho v_p^2}\cdot\frac{1}{r^{(i)}}\{\gamma_k^{(i)}\mu_k^{(i)}\}\cdot(\gamma_l^{(i)}n_l)(\gamma_m^{(i)}v_m) \quad (i=1, 2, \cdots, N) \tag{10}$$

Correction of amplitude at detecting point $R^{(i)}$ is as follows;

$$R^{(i)}=\frac{u_{k(P)}{}^{(i)}\mu_k^{(i)}}{\frac{1}{r^{(i)}}\{\gamma_k^{(i)}\mu_k^{(i)}\}}=A(\gamma_l^{(i)}n_l)(\gamma_m^{(i)}v_m)$$
$$=A(\gamma_1^{(i)}n_1+\gamma_2^{(i)}n_2+\gamma_3^{(i)}n_3)\cdot(\gamma_1^{(i)}v_1+\gamma_2^{(i)}v_2+\gamma_3^{(i)}v_3) \quad (i=1, 2, \cdots, N) \tag{11}$$

Eq. (11) is simultaneous equation of the number of detecting point N having the unknown A, n_1, n_2, n_3, v_1, v_2, v_3. But, if γ, n, v represent with unit vector and n, v with spherical coordinate, angle (θ_n, ϕ_n), (θ_v, ϕ_v) and amplitude A can be represented with simulataneous equation. Therefore, the direction of dislocation surface v and dislocation direction n which is applied direction of force can be determined from amplitudes detected by transducers more than five channels and accurate source coordinates.

Tensile dislocation

Tensile dislocation take place when v and n are aligned in same direction making $v_in_i=1$, and the component of dislocation relating to longitudinal wave is calculated as eq. (12).

$$u_k\gamma_k=\frac{\mu\cdot U}{4\pi\rho v_p^2}\cdot\frac{1}{r}\left[\frac{2\nu}{(1-2\nu)}+2(\gamma_iv_i)^2\right]\delta\left(t-\frac{r}{v_p}\right) \tag{12}$$

If tensile dislocation is considered as Fig. 3 it can be expressed as eq. (13) below;

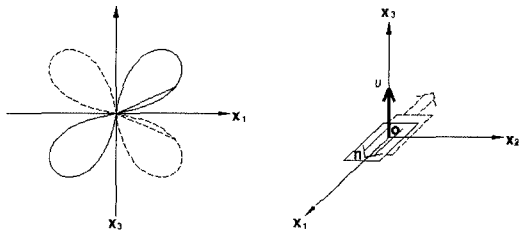

(a) dislocation model (b) radiation pattern

Fig. 2. Shear dislocation model and its radiation pattern.

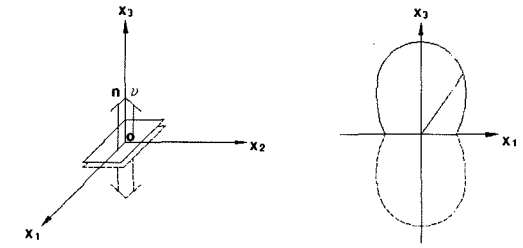

(a) dislocation model (b) radiation pattern

Fig. 3. Tensile dislocation model and its radiation pattern.

$$u_{(P)}=\frac{2v}{(1-2v)}+2\cos^2\theta \tag{13}$$

Amplitude of the first motion of longitudinal wave in eq. (12) is as follows;

$$u_{k(P)}{}^{(i)}\mu_k^{(i)}=\frac{2\mu\cdot U}{4\pi\rho\upsilon_p^2}\cdot\frac{1}{r^{(i)}}\{\gamma_k^{(i)}\mu_k^{(i)}\}\cdot\left[\frac{v}{(1-2v)}+(\gamma_l v_l)^2\right] \tag{14}$$

$$(i=1, 2, \cdots, N)$$

Correction of amplitude at detecting point $R^{(t)}$ as well shear dislocation theory is as follows;

$$R^{(t)}=\frac{u_{k(P)}{}^{(i)}\mu_k^{(i)}}{\frac{1}{r^{(i)}}\{\gamma_k^{(i)}\mu_k^{(i)}\}}=A\left[\frac{v}{1-2v}+(\gamma_l^{(i)}n_l)^2\right] \tag{15}$$

$$=A\left[\frac{v}{1-2v}+(\gamma_1^{(i)}n_1+\gamma_2^{(i)}n_2+\gamma_3^{(i)}n_3)^2\right]$$

$$(i=1, 2, \cdots, N)$$

Our view thus far tells us that it is possible to represent radiation patterns particular to each dislocation model i. e. source mechanism. In general crack patterns within rock are classified as tensile crack, shear crack and combined crack of tension and shear, and it is considered that tensile dislocation causes tensile crack and shear dislocation causes shear crack.

Experimental Programs

Preparation of specimens

Mortar and Geochang granite in Korea were selected specimen to be used in this research. Physical properties of specimen used are as shown in Table 1.

Table 1. Physical properties of samples

Origins of samples	Geochang granite	Mortar
Unit weight (KN/m^3)	25.81	20.93
Longitudinal wave velocity (m/sec)	4850	3850
Porosity (%)	0.87	-
Uni. compressive strength (MPa)	170	24
Young's modulus (×10^4 MPa)	5.18	2.36
Poisson's ratio	0.19	0.18

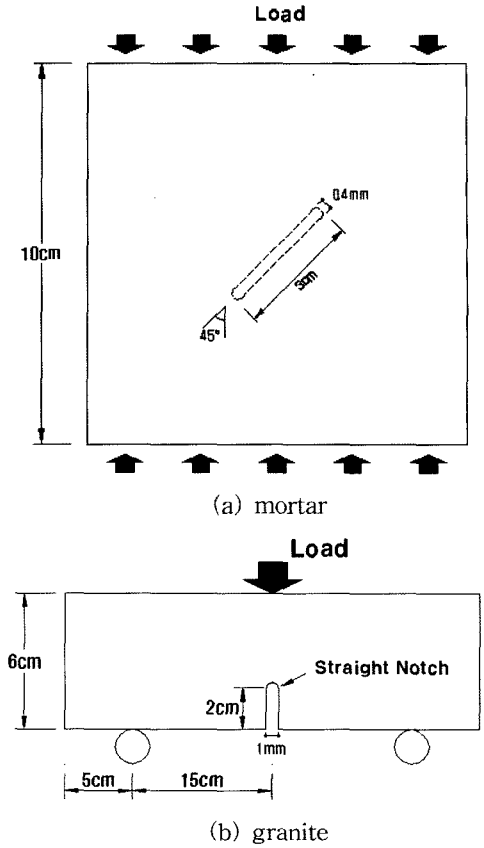

Fig. 4. Configurations of rock and mortar specimen.

Notch of rock specimen was made by diamond cutter for three point bending test, of which size and shape are as shown in Fig. 4(a). Rock specimen is 6×6×40 cm in its size, which has vertical notch at the center, sized 1 mm wide and 2 cm long, which was intended to induce tensile crack. Mortar specimen shown in Fig. 4(b) is 10×10×10 cm in its size, which has at the center artificial slit sloped in 45° with axis of load, sized 3 cm long and 0.4 mm wide. Mixture of the mortar in this case was designed to have proportion in weight that water, cement and sand is 0.6, 1.0 and 2.0 respectively.

The reason for forming artificial crack in the specimen is to find out characteristics of source mechanism of micro-crack based on the adoptability of dynamic model of dislocation which could be obtained from the source location determined.

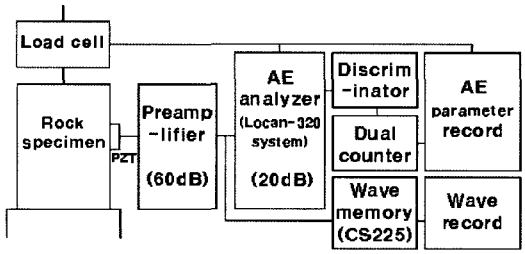

Fig. 5. Block diagram of experimental setup for monitoring.

Test apparatus and monitoring system of acoustic emission

Test apparatus used is SFM model manufactured by UNITED Co. in USA. Instrument for acoustic emission measurement is model LOCAN-320 of PAC Co. in USA, which is capable of processing 2 to 14 signals. Transducer used for analyzing source location of micro-crack at loading is model WD-A having resonance frequency of 550 KHz of PAC Co. Meanwhile, acoustic emission waveform emitted out of 6 channels, after recording by waveform recorder (model CS225), were saved in the form of digital data in a personal computer. Fig. 5 briefly depicts monitoring system of acoustic emission.

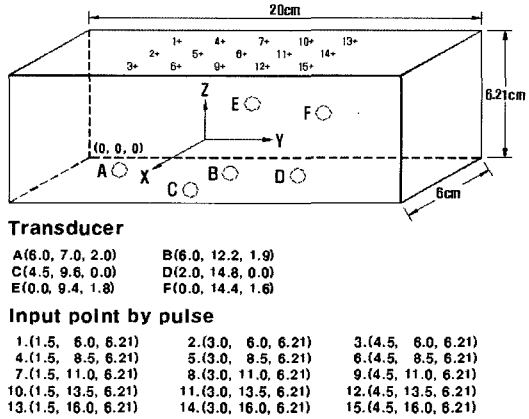

Fig. 6. Transducers array and input points.

Results

After source location of acoustic emission is determined, only the first motion of longitudinal wave of waveform arrived to the transducer was applied to review dislocation of point forces, tension and shear forces.

Dislocation result from point forces

As shown in Fig. 6, by means of pulse input using the transducer R15, point forces having ver-

Table 2. Source coordinates and the first amplitude of longitudinal wave detected by transducers (x, y, z coordinate).

Point of pulse input	Source (cm)						First amplitude of longitudinal wave detected by transducers (mV)					
	Coordinates of pulse input point			Coordinates calculated from the least square method								
	X	Y	Z	X	Y	Z	A	B	C	D	E	F
1	1.5	6.0	6.21	1.80	6.21	5.01	296	24	424	96	160	16
2	3.0	6.0	6.21	3.41	5.60	6.77	360	104	508	72	236	16
3	4.5	6.0	6.21	4.38	5.81	6.60	304	56	524	64	236	24
4	1.5	8.5	6.21	1.72	8.32	5.82	328	280	516	220	376	32
5	3.0	8.5	6.21	3.07	8.35	6.23	304	212	532	172	400	40
6	4.5	8.5	6.21	4.44	8.68	5.93	236	156	532	156	392	40
7	1.5	11.0	6.21	1.36	10.73	6.14	148	376	500	400	244	72
8	3.0	11.0	6.21	3.06	10.90	6.38	140	408	524	408	328	96
9	4.5	11.0	6.21	4.57	10.97	6.45	112	336	532	376	392	120
10	1.5	13.5	6.21	1.75	12.98	5.41	64	16	400	456	104	136
11	3.0	13.5	6.21	3.41	13.30	6.15	48	320	448	448	120	144
12	4.5	13.5	6.21	4.39	13.06	5.88	40	312	508	448	180	180
13	1.5	16.0	6.21	2.05	14.85	4.96	32	220	212	456	40	136
14	3.0	16.0	6.21	3.14	15.00	5.02	32	180	236	456	56	160
15	4.5	16.0	6.21	4.26	14.94	4.74	16	140	292	456	88	172

tical movement was imposed. And elastic wave propagated through the transducer WD-A attatched at the surface of granite specimen was monitored to automatically record its waveforms to the disc. Now the 3-dimensional source location can be obtained by determining the arrived time out of waveforms recorded, and by applying this with the only consideration of the first motion of longitudinal wave as Table 2 with the eqs. (3) and (5), direction of point forces can be obtained as shown in Fig. 7.

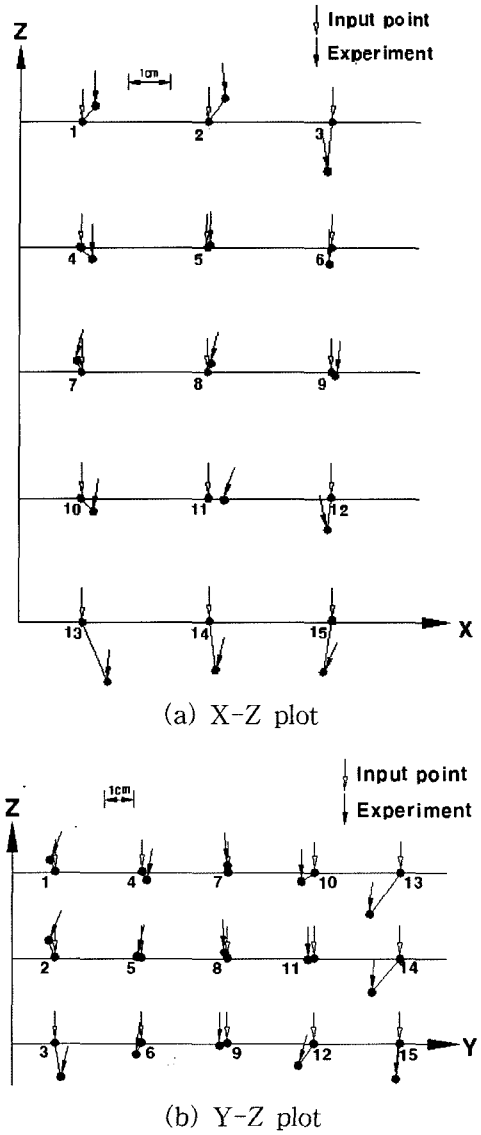

Fig. 7. Detected sources and direction of point forces calculated.

Looking at it from X-Z plane in Fig. 7(a), at the points of force after the 10th point force, source location errors are revealed to be rather big ranging 0.4 to 0.6 cm, and errors in directions of point force were also revealed to be greater than at other points of force. On the other hand, source location errors at the points of force before 9th point force, except at the 1st, 2nd and 3rd points, were relatively minor ranging 0.07 to 0.4 cm, and directions of point force of them obtained were almost same as their actual directions.

Looking at it from X-Z plane, it was observed that errors related to the points at the left and right end side of the plane, i. e. points 1, 2, 3, 13, 14 and 15, are greater than to other points.

Therefore it comes to a conclusion if error in analyzing source location is small enough, direction of point force accordingly defined is almost identical to that of input points. It makes thus certain that determination of accurate source location is the key factor for the study on the mechanism of micro-crack within the material.

Dislocation of shear force and tension

In order to compare the micro-crack by shear force and tension in this study, explanation will be

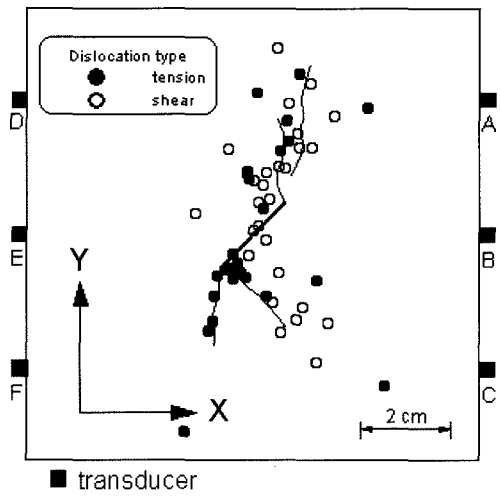

Fig. 8. Sources and dislocation type in mortar.

made first in case with mortar specimen, in which propagation velocity of longitudinal wave is more or less 3,935 m/sec in all direction with only 2 to 3% of minor deviation between each different direction.

The dislocation of shear force and tension are as shown in Fig. 8. As it has been reviewed in radiation theory of shear dislocation, because in case of the direction of dislocation and dislocation surface associated is in the same direction, the direction of dislocation and dislocation surface calculated from actual analysis deviates within ±30°, that dislocation was defined as for shear crack. If the deviation is slightly beyond ±30°, analysis was made based on radiation theory of tensile dislocation. If in case the deviation is greater than the above two cases, then that dislocation was defined as for mixed crack.

In the above figure, sources are intensely distributed at the upper side, lower side, and topside of the slit. Out of total 66 sources 28 events showed result of shear dislocation and 24 events result of tensile dislocation. The result explains that shear crack face is formed around the slit face, so it comes to our knowledge that the direction of shear crack and force resulted from this test are well in square with the result of Ohtsu's test. Result of the analysis of shear dislocation tells us that micro -crack takes place mostly at the lower side of the slit and partly at upper side and topside of the slit. When the test result on shear dislocation was delineated in rose diagram, the direction of shear dislocation were revealed to be prevailing within the range 30° to 47° and partly around 125° clockwise at loading axis, while the direction of dislocation surface were prevailing at 45° and sparsely at 145° as shown in Fig. 9(a). That means the direction of crack and crack surface in case of shearing almost coincide one another within a slight deviation. The same was found to be true in crack formation at the upper part of the slit.

On the other hand, tensile dislocation surface directing in 149° in average intersects with shear dislocation surface in around 86° thus to be perpendicular to the slit surface as Fig. 9(b). Now all these results make it obvious that the results are well in match with micro-crack surface at the lower end of the slit.

By analogy to the above, stress behavior within the mortar specimen is in first assumed to be that tensile crack at both end of the slit takes place by tensioning and, from the moment that the slit surface is closed, shear crack by sliding will take

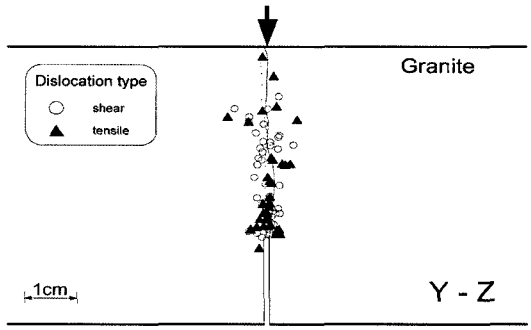

Fig. 10. Sources and dislocation type in three point bending test.

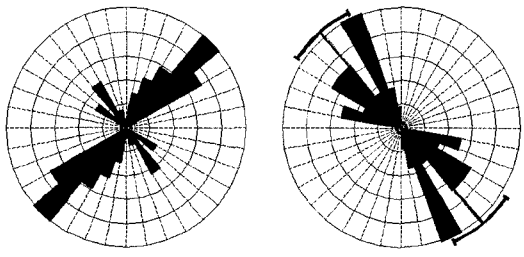

Fig. 9. Rose diagram of the direction dislocation surface in mortar.

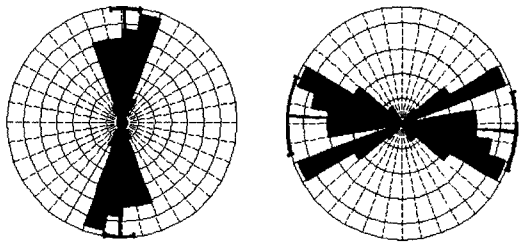

Fig. 11. Rose diagram of the direction of dislocation in granite.

place.

Fig. 10 shows dislocation distribution obtained from three point bending test with granite specimen. It is observed that tensile dislocation largely distributes around the edge of notch and shear dislocation in general distributes at the edge of notch and 2cm above the edge. Rose diagram for the direction of dislocation is as shown in Fig. 11. The direction of shear dislocation almost parallels with direction of loading axis and the direction of tensile dislocation in general intersects with direction of loading axis in more or less 185°. It is concluded that shear force behaves itself to direct to be parallel to the direction of loading axis and tensile force apply to be perpendicular to the direction of loading axis, for the failure takes place along the edge of notch.

Fig. 12 shows the relationship between the ratio for maximum load and the ratio for total events, where no event was found when loading is less than 60% of maximum load. In order to get clear distinction in amplitude of first motion of longitudinal wave and to determine micro-crack mechanism, threshold voltage was raised to 100 mV.

When it is looked in macroscopic point of view, failure by tensile force breaks out, yet , looking at individual cracks within rock, failure is more prominently of shear dislocation i. e. shear crack.

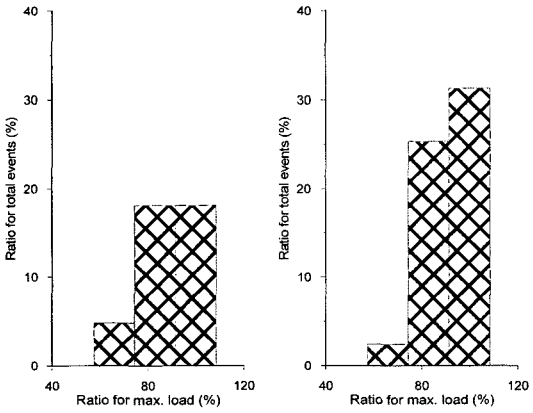

Fig. 12. Frequency of events for tensile and shear dislocation in granite.

It was found that at the initial stage of crack there happen slightly more tensile cracks than shear cracks, but as the loading approaches to the maximum load frequency of shear cracks increase. Such is because as the micro-cracks within rock approach to the maximum load, sliding of crack surfaces due to connecting and expanding between the cracks becomes increasingly activated.

As it has been so far mentioned, it is proved to be true that crack orientation in rock is well in coincidence with the direction of dislocation surface obtained from radiation pattern. Therefore, it is considered that useful information for understanding micro-crack mechanism in rock could be obtained by applying radiation pattern.

Discussion

So far, we have found, by applying the least square method, source location from the longitudinal waves of acoustic emission through rupture tests with specimen prepared to study micro-crack mechanism within the material, and found distance to the transducer by means of calculating back from the source location, and applied radiation pattern regarding shear dislocation and tensile dislocation. Result of analysis showed that the orientation of dislocation surfaces due to shear dislocation and tensile dislocation squares with crack direction visually observed.

If we apply radiation pattern through reverse transformation after finding source location through measuring acoustic emission, shear crack and tensile crack in real rock mass could be foreseen although they could not visually be identified. Crack due to tensile dislocation is considered to direct itself perpendicularly to the dislocation direction - vector sum of three directional components of force, while crack due to shear dislocation, which is led by sliding, will direct in parallel with the dislocation direction. Such results were apparently observed through rupture tests with mortar and rock specimen.

In this study specimens were so prepared that the shape of dislocation and dislocation surface

could be foreseen. In case of three point bending test, when it is looked upon macroscopic point of view, failure is predominantly owing to tensile micro-crack. However, the result of applying radiation pattern shows that failure is actually from mixture of tension and shear mechanism. This result is well in square with the result of study by Falls *et al.*, (1991) where the shape and orientation of micro-cracks were determined by means of characteristics of the first motion of longitudinal wave obtained through Brazilian indirect tension test. Study by Falls *et al.*, (1991) reports that micro-crack in rock take place in almost equally proportion of tensile dislocation and shear dislocation. It also proved that events of acoustic emission distribute densely at the zone where the biggest difference between the maximum principal stress and the minimum principal stress in rock exists. Therefore, it could likewise be explained that the reason why the source distributed densely around the edge of notch and the end of slit because the difference between the two principal stresses was the greatest. If we assume that at the location where source is densely distribute in any rock mass the difference between the two principal stresses are great, this fact could be used as useful means for founding the beginning point of the crack.

Conclusion

Laboratory test on acoustic emission was performed with two different specimens of granite containing straight notch at middle and mortar containing slit. By analyzing characteristics of the first motion of longitudinal wave that is propagated from sources, and adopting radiation pattern theory based on dynamic elastic theory, study on micro-crack mechanism was carried out.

It was testified that, using the distance from the source location to the transducer upon the source location is determined, incidence angle of the wave and the first motion of longitudinal wave, identification of shear dislocation and tensile dislocation i. e. shear crack and tensile crack is possible.

Tests performed for the study with respect to this thesis limits to the tests with mortar and rock specimens which were prepared to study on source mechanism of micro-crack. However, the result of this research may as well be referred to when further study on acoustic emission by testing with other rock specimens or real rock mass in field.

References

Ko, H. J., 1983, A Study on A.E. Source Location of Cylindrical Specimen and Plate with s Circular Hole under Uniaxial Compressive Stress, Master of Science Thesis, Seoul University, 44p.

Kim, H., 1990, A Study on the Mechanism of Hydraulic Fracturing of the Inclined Borehole of the Rock Model and on the Source Location Using Acoustic Emission, Master of Science Thesis, Seoul University, 66p.

Aki, K. and Richards, P. G., 1980, Quantitative Seismology Theory and Method, Vol. 1, W. H. Freeman and Company, Sanfransisco.

Leighton, F., and Duvall, W. L., 1972, A Least Squares Method for Improving the Source Location of Rock Noise, United States Bureau of Mines, RI 7626.

Lee, K. S., 1996, 3D Source Location using the Acoustic Emission Considering the Velocity Anisotropy in rock Master of Science Thesis, Seoul University, 65p.

Ohtsu, M., 1983, Acoustic Emission Source Kinematics Based on the Moving Dislocation Theory, J. of Acoustic Emission, Vol. 2, No. 3, pp.151-158.

Falls, S. D. T., Chow, R. P., Young, and Hutchins, D. A., 1991, Acoustic Emission Analysis and Ultrasonic Velocity Imaging in the Study of Rock Failure, Acoustic Emission: Current Practice and Future Directions, ASTM STP 1077, W. Sachse, J. Roget, and K. Yamaguchi, Eds., ASTM, Philadelphia.

2006년 4월 10일 원고접수, 2006년 6월 15일 게재승인

Sang-Eun Lee
Sambo Engineering Co., Ltd.
138-834 Sambo Bldg. 200-2, Bang i-1Dong,
Songpa-Gu, Seoul, Korea
Tel: 02-3433-3084
Fax: 02-3433-3192
e-mail: lee9367@hanmail.net